Modulatory Effect of Glycated Collagen on Oral Streptococcal Nanoadhesion

Journal of Dental Research
2021, Vol. 100(1) 82–89

DOI: 10.1177/0022034520946320
journals.sagepub.com/home/jdr

C.M.A.P. Schuh[1], B. Benso[2], P.A. Naulin[3], N.P. Barrera[3], L. Bozec[4], and S. Aguayo[2,5]

Abstract

Biofilm-mediated oral diseases such as dental caries and periodontal disease remain highly prevalent in populations worldwide. Biofilm formation initiates with the attachment of primary colonizers onto surfaces, and in the context of caries, the adhesion of oral streptococci to dentinal collagen is crucial for biofilm progression. It is known that dentinal collagen suffers from glucose-associated crosslinking as a function of aging or disease; however, the effect of collagen crosslinking on the early adhesion and subsequent biofilm formation of relevant oral streptococci remains unknown. Therefore, the aim of this work was to determine the impact of collagen glycation on the initial adhesion of primary colonizers such as *Streptococcus mutans* UA159 and *Streptococcus sanguinis* SK 36, as well as its effect on the early stages of streptococcal biofilm formation in vitro. Type I collagen matrices were crosslinked with either glucose or methylglyoxal. Atomic force microscopy nanocharacterization revealed morphologic and mechanical changes within the collagen matrix as a function of crosslinking, such as a significantly increased elastic modulus in crosslinked fibrils. Increased nanoadhesion forces were observed for *S. mutans* on crosslinked collagen surfaces as compared with the control, and retraction curves obtained for both streptococcal strains demonstrated nanoscale unbinding behavior consistent with bacterial adhesin-substrate coupling. Overall, glucose-crosslinked substrates specifically promoted the initial adhesion, biofilm formation, and insoluble extracellular polysaccharide production of *S. mutans*, while methylglyoxal treatment reduced biofilm formation for both strains. Changes in the adhesion behavior and biofilm formation of oral streptococci as a function of collagen glycation could help explain the biofilm dysbiosis seen in older people and patients with diabetes. Further studies are necessary to determine the influence of collagen crosslinking on the balance between acidogenic and nonacidogenic streptococci to aid in the development of novel preventive and therapeutic treatment against dental caries in these patients.

Keywords: atomic force microscopy, bacterial adhesion, biofilms, aging, dental caries, *Streptococcus mutans*

Introduction

Despite current efforts, biofilm-mediated oral diseases such as dental caries and periodontal disease continue to be highly prevalent worldwide (Kassebaum et al. 2014; Vos et al. 2017). Oral biofilms are complex communities of microorganisms attached to surfaces and embedded in extracellular polysaccharide substance (EPS; Donlan 2002; Flemming and Wingender 2010). Although biofilm formation is an intricate multistage process, it is initiated by the attachment of early bacterial colonizers, such as streptococci, to dental substrates (Hojo et al. 2009).

Within this context, it is understood that the balance among the different microbial species cohabiting within biofilms is important for preventing dysbiosis and maintaining oral health (Marsh 1994; Takahashi and Nyvad 2008). Specifically, the balance between *Streptococcus sanguinis* and *Streptococcus mutans* is an important factor in the pathogenesis of dental caries (Zheng et al. 2011; Zhu et al. 2018; Guo et al. 2019). *S. sanguinis* is a commensal species regarded as one of the early colonizers of dental substrates (with *Streptococcus mitis, Streptococcus oralis*, and *Actinomyces* spp., among others), as it expresses multiple microbial adhesins facilitating its adhesion to surfaces (Kreth et al. 2009; Zhu et al. 2018). *S. mutans*, however, is an acidogenic strain, and its increased prevalence within biofilms can lead to progressive demineralization of the surface layers of the tooth (Loesche 1986). Furthermore, oral streptococci express several collagen-specific surface adhesins, such as wapA, spaP, and cnm (Switalski et al. 1993; Ajdic et al. 2002; Sato et al. 2004; Avilés-Reyes et al. 2017). These collagen-specific adhesins have been shown to play an

[1]Centro de Medicina Regenerativa, Facultad de Medicina Clínica Alemana–Universidad del Desarrollo, Santiago, Chile
[2]School of Dentistry, Faculty of Medicine, Pontificia Universidad Católica de Chile, Santiago, Chile
[3]Department of Physiology, Faculty of Biological Sciences, Pontificia Universidad Católica de Chile, Santiago, Chile
[4]Faculty of Dentistry, University of Toronto, Toronto, Canada
[5]Institute for Biological and Medical Engineering, Schools of Engineering, Medicine and Biological Sciences, Pontificia Universidad Católica de Chile, Santiago, Chile

A supplemental appendix to this article is available online.

Corresponding Author:
S. Aguayo, School of Dentistry, Faculty of Medicine, Pontificia Universidad Católica de Chile, Avenida Libertador General Bernardo O'Higgins #340, Santiago, Santiago Province, Chile 8320000.
Email: sebastian.aguayo@uc.cl

important role in the progression of bacteria into the collagen-rich dentinal layer, as well as in the progression of root caries, especially in older people and patients with diabetes (Takahashi and Nyvad 2016).

Type I collagen, the most abundant structural protein in the human body (Gelse et al. 2003), has a hierarchical arrangement originating from the polymerization of collagen molecules into fibrils. Type I collagen is also subjected to intermolecular crosslinking due to posttranslational modifications. However, in its mature fibrillar form, collagen is also subjected to nonenzymatic glycation resulting from natural aging (Nass et al. 2007). Glycation is driven by the Maillard reaction, in which the aldehyde group of reducing sugars (e.g., glucose) binds to ε-amino group of proteins to form a Schiff base. Following a time-dependent rearrangement, the Schiff base becomes an Amadori product, which in turn is converted into stable substances through oxidation, dehydration, and condensation (Collier et al. 2016). Among the slower-forming advanced glycation end products (AGEs) are glucosepane and pentosidine, while oxidative intermediaries such as glyoxal and methylglyoxal (MGO) react in a manner of hours and days. Besides being an important mechanism of the aging process, collagen glycation is relevant in pathologic conditions such as diabetes mellitus, due to the increased levels of glucose within tissues (Snedeker and Gautieri 2014). Recent research has suggested that dentin is also affected by AGE-mediated crosslinking, as increased levels of AGEs were found in older people (Shinno et al. 2016; Greis et al. 2018). However, the influence of these glycation-induced collagen modifications on oral streptococcal attachment onto surfaces and subsequent biofilm formation remains unknown. Combining early adhesion data with subsequent biofilm growth observations could increase our understanding of the mechanisms behind the initial stages of oral streptococcal biofilm formation on type I collagen surfaces and play a crucial role in future biofilm research.

Therefore, the aim of this work was to determine the impact of collagen glycation on the early adhesion of *S. sanguinis* and *S. mutans* cells onto surfaces, as well as its effect on the early stages of streptococcal biofilm formation in vitro.

Materials and Methods

Collagen Substrates and Glycation

Type I rat tail collagen gels (3 mg/mL; Gibco, Life Technologies) were prepared by combining ice-cold collagen, 10 × PBS, dH_2O, and 1 N NaOH to obtain final concentrations of 1-mg/mL collagen, 1 × PBS, and 8.3mM NaOH and pH 7.4. Collagen gels (50 µL) were incubated in a 96-well plate for 30 min at 37 °C. Subsequently resulting gels were covered with 100-µL PBS to avoid dehydration and immediately used for experiments. After removal of PBS supernatants, in vitro crosslinking of collagen gels was obtained by incubating gels with 100 µL of 500mM glucose (D-[+]-Glucose; Sigma) or 10mM MGO (Sigma) for 5 d at 37 °C, and 20mM aminoguanidine (AMG; Sigma) was used as a control to inhibit MGO crosslinking (Chong et al. 2007).

Assessment of In Vitro Collagen Glycation

The autofluorescence of collagen crosslinking was assessed with a multimodal microplate reader (Synergy HT, Biotek; Francis-Sedlak et al. 2009). Crosslinked collagen gels were measured at 24-h intervals for 5 d (excitation/emission: 360 nm/460 nm) and as compared with control ($n = 3$, in technical triplicates). To determine collagen modification by glycation, SDS-PAGE (sodium dodecyl sulfate–polyacrylamide gel electrophoresis) was performed. Collagen gels were mechanically fragmented with pellet pestles (Sigma) and lysed with radioimmunoprecipitation assay buffer. Samples were separated in a 6% polyacrylamide gel and subsequently visualized with Coomassie blue. Scanning electron microscopy (SEM) was employed to confirm morphologic modifications of the collagen network. Samples were fixed with 2.5% glutaraldehyde for 12 h, followed by ethanol series dehydration and hexamethyldisiloxane-assisted drying. After gold sputter coating, collagen samples were visualized with a scanning electron microscope (JSM-IT300 LV; JEOL).

Atomic Force Microscope Imaging and Nanomechanics of Collagen Gels

Collagen gel samples were washed 3 times in dH_2O after glycation and physisorbed onto 9-mm-diameter glass coverslips. TAP300GD-G cantilevers (k~40 N/m, ~300 kHz; Budget Sensors) were calibrated in air with an atomic force microscope (AFM; MFP 3D-SA, Asylum Research) and employed in intermittent contact (AC mode) to obtain a minimum of three 5 × 5–µm scans of collagen gels at 512 × 512 pixels. Subsequently, force-distance curves were obtained on the length of individualized fibers with an indentation force of 30 nN (10 force-distance curves per fiber, 3 to 5 fibers per image). Young's moduli were calculated by employing the Derjaguin, Muller, and Toporov model with proprietary Asylum Research AFM software (v. 16.10.211), and nanoscale roughness averages of collagen surfaces were determined from 5 × 5–µm height images with the WSxM 5.0 software.

Bacterial Strains

S. mutans UA159 (ATCC 700610) and *S. sanguinis* SK 36 (Xu et al. 2007) were maintained at 37 °C and 5% CO_2 on brain-heart infusion (BHI) agar (BD) and trypticase soy agar supplemented with 5% blood, respectively.

AFM Probe Functionalization for Single-Bacterium Adhesion Experiments

For AFM probe functionalization, an adaptation of a previously published approach was used (Wang et al. 2019). Briefly, BL-TR400PB iDrive AFM cantilevers ($k \sim 0.09$ N/m, ~32 kHz; Asylum Research) were functionalized by incubation with a 50-µL droplet of 0.01M poly-L-lysine solution (Sigma) for 2 min. After air-drying, a 50-µL droplet of bacteria solution (~1×10^6 CFU/mL) in PBS was incubated on the cantilever for

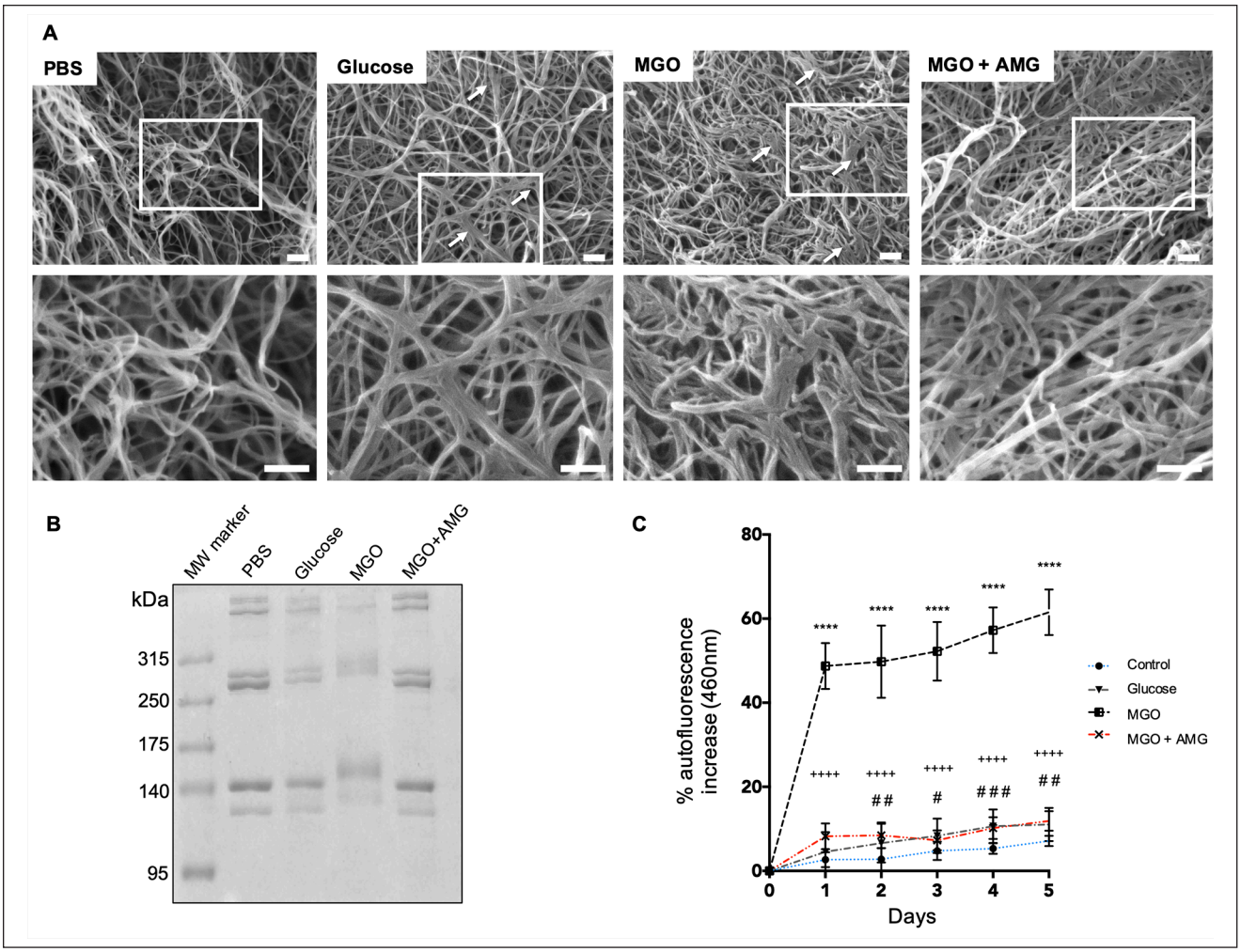

Figure 1. Morphologic and biochemical characterization of control and AGE-crosslinked type I collagen substrates. (**A**) Scanning electron microscopy images of control collagen (in PBS) and collagen crosslinked with 500mM glucose, 10mM MGO, or 10mM MGO + 20mM AMG (scale bar ≙ 1 µm). Arrows represent areas of fibril bunching and clumping, observed as an effect of crosslinking. (**B**) SDS-PAGE of control collagen and collagen treated with glucose, MGO, or a combination of MGO and AMG. (**C**) Collagen AGE accumulation expressed as a percentage of autofluorescence increase (460 nm) over a 5-d incubation period. Values are presented as mean ± SD. *$P<0.05$. **$P<0.01$. ****$P<0.0001$. Two-way analysis of variance. $n=3$. Three technical replicates per group per independent n. Statistical significance between *MGO and controls, $^{+}$MGO + AMG and controls, and $^{\#}$glucose and controls. AGE, advanced glycation end product; AMG, aminoguanidine; MGO, methylglyoxal; PBS, phosphate-buffered saline.

2 min, gently washed with PBS, and immediately transferred to the AFM to avoid dehydration. Force spectroscopy experiments were performed in PBS in iDrive mode with a maximum loading force of 200 pN and speed of 0.5 Hz. Adhesion between probes and collagen was recorded with dwelling times of 0 s and 5 s, with 50 force curves across 5 random locations, for a total of 250 force curves per condition. Maximum adhesion values were extracted with proprietary Asylum Research AFM software.

Biofilm Growth Experiments and Characterization

Prior to biofilm formation experiments, gels were washed 3 times with PBS, incubated in 100 µL PBS for 24 h at 4 °C, and again washed 3 times in PBS to remove any residual crosslinking agents potentially affecting biofilm growth. Twenty-four-hour bacterial colonies were inoculated in BHI broth, adjusted to McFarland 0.5, and adjusted to 5×10^6 CFU/mL (Clinical and Laboratory Standards Institute 2014). Bacteria were subsequently grown on collagen substrates in a total volume of 100-µL BHI supplemented with 1% sucrose for 24 h at 37 °C and 5% CO_2. After incubation, gels were washed 3 times with PBS to remove unattached bacteria and immediately processed for characterization and quantification. Biofilm biomass was determined by crystal violet (0.01%) staining as previously described (Schuh et al. 2019). For SEM, biofilm-coated gels were prepared as described and imaged with a scanning electron microscope (VP1400; LEO).

Confocal Laser Scanning Microscopy of Biofilms

Bacteria were grown as indicated, with the addition of 2.5µM Cascade Blue–conjugated dextran (Thermo Fisher) for 24 h.

After removal of unattached bacteria, biofilms were stained with Live/Dead BacLight (Thermo Fisher) by incubation in a 1:1 ratio of SYTO9 and propidium iodide for 30 min at room temperature, protected from light. Samples were washed 3 times with PBS, and imaging was performed with an LSM 880 ZEISS microscope with Airyscan detection, and Z-stacks and 3-dimensional reconstructions were obtained with the ZEISS ZEN (v. 3.1) software. EPS production was calculated as the mean intensity index for Cascade Blue in the basal portion of the attached biofilms for all 3 conditions.

Biofilm EPS Estimation

After growth, 24-h biofilms were sonicated and centrifuged at 10,000*g* for 5 min at 4 °C. Supernatants were precipitated into ice-cold 100% ethanol to extract soluble EPS (SEPS). Pellets were then resuspended in 400-µL 1M NaOH and centrifuged for 5 min, and supernatants were reprecipitated into ice-cold 100% ethanol to extract insoluble EPS (IEPS). SEPS and IEPS samples were placed at −20 °C until analysis. After being centrifuged and washed with 70% ethanol twice, a phenol-sulfuric method was used for subsequent quantification of carbohydrate content as previously described (DuBois et al. 1956; standard: glucose). Results were normalized to biofilm wet weight (Oliveira et al. 2017).

Statistical Analysis

Statistical analyses were obtained with Prism (v. 6; GraphPad) and Stata (v. 10.0; StataCorp). The component analysis and data with large residual errors were defined as outliers. Results were expressed as mean and standard deviation, box plots, or histograms, and statistical analysis was performed by *t* test, analysis of variance, or Kruskal-Wallis, with significance at $P < 0.05$.

Results and Discussion

Glycation Induces Morphologic and Biochemical Modifications in Collagen Fibrils

In assessing the morphology of collagen matrices in the presence of crosslinking agents, we found that glucose and MGO generated important changes to the fibrillar structure (Fig. 1A). SEM imaging revealed that treatment with glucose altered the diameter and density of collagen fibrils as compared with controls. Furthermore, incubation with MGO strongly altered the morphology of the matrix, with significant areas of fibril clumping; however, AMG appeared to partly inhibit MGO-associated morphologic changes. These results were consistent with the SDS-PAGE (Fig. 1B), which demonstrated a slower migration of glucose- and MGO-crosslinked collagen as compared with the controls.

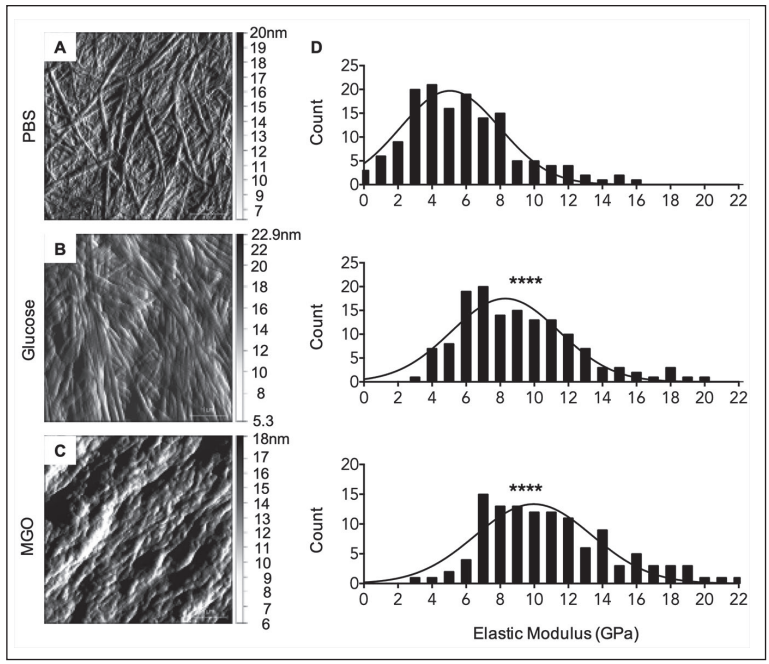

Figure 2. AFM nanometric and nanomechanical characterization of control and glucose- and MGO-crosslinked collagen. (**A**–**C**) AFM height topography scans (5 × 5 µm) of control, glucose-, and MGO-modified collagen gels, respectively. (**D**) Histograms of reduced modulus obtained with the DMT model for control, glucose-, and MGO-modified collagen gels, respectively. Each histogram represents 150 indentation points on the surface of individualized collagen fibers, across 3 independent collagen gels per group. ****$P < 0.0001$. Kruskal-Wallis test. MGO and glucose vs. control. AFM, atomic force microscopy; DMT, Derjaguin, Muller, and Toporov; MGO, methylglyoxal; PBS, phosphate-buffered saline.

Crosslinking was also quantified via autofluorescence, and it was observed that MGO significantly increased collagen crosslinking by about 50% after 24 h (Fig. 1C). Glucose displayed a linear increase in AGE-associated fluorescence until day 5 but never reached the levels of MGO crosslinking. In all cases, including the control, there was a time-dependent increase in crosslinking throughout the assay. These results are consistent with previous reports showing that MGO is a faster AGE generator than glucose (Nevin et al. 2018). Overall, glucose seems to have a milder, more time-dependent effect, while MGO treatment appears to mimic the process of chemical crosslinking via external agents (Akhshabi et al. 2018).

Nanomechanical Properties of Collagen Fibrils as a Function of Glycation

Nanocharacterization of physisorbed collagen gels confirmed changes in the ultrastructure of collagen fibrils as a function of glycation (Fig. 2A–C). Regarding nanomechanical properties, glucose and MGO significantly increased the elastic modulus of collagen as compared with the control (Fig. 2D). This effect was more pronounced in MGO-treated gels, with a median elasticity value of 10.36 GPa, as opposed to 5.45 GPa and 8.69 GPa for control and glucose-treated collagen, respectively. These

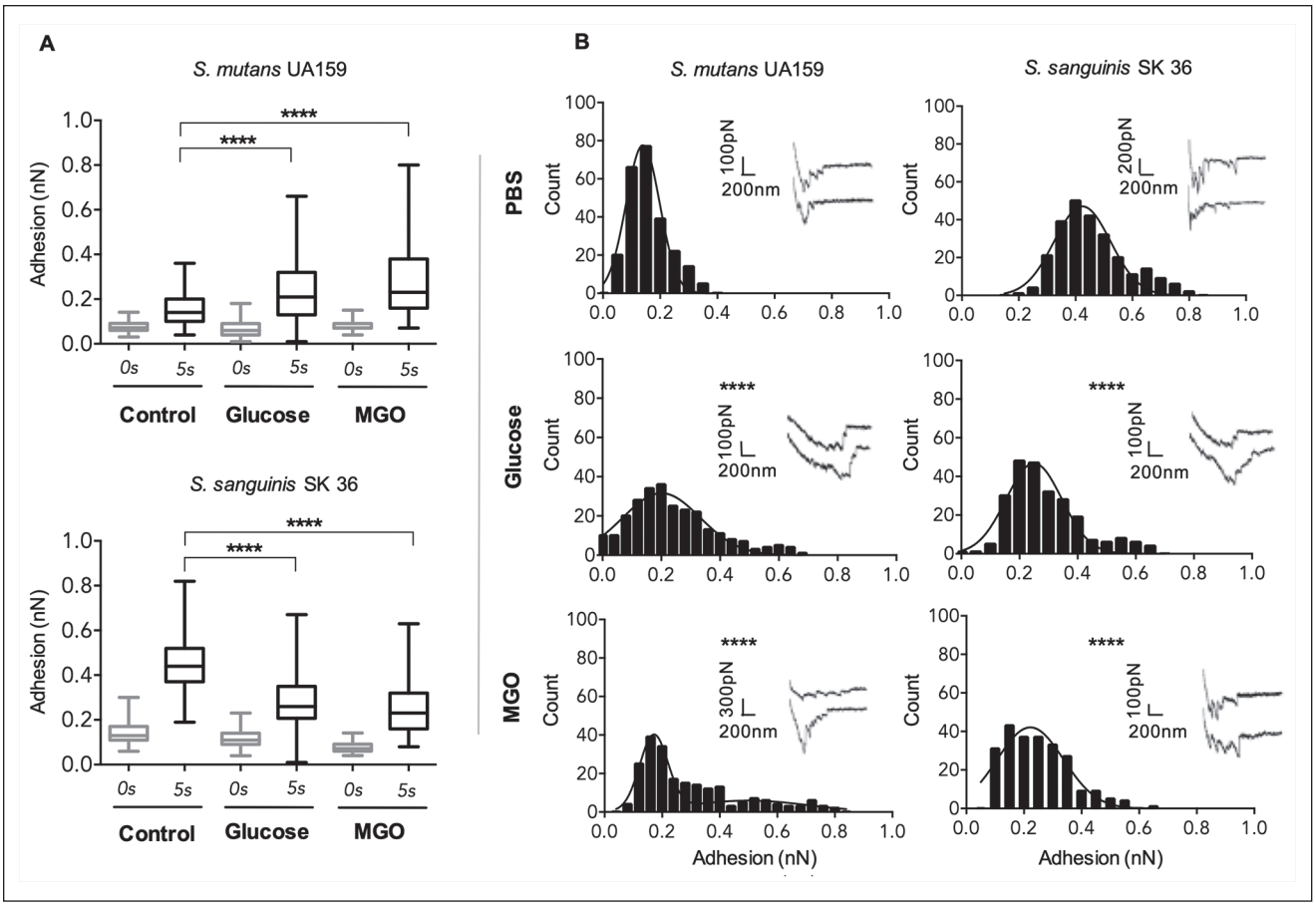

Figure 3. Nanoadhesion of *Streptococcus mutans* UA159 and *Streptococcus sanguinis* SK 36 to crosslinked collagen surfaces probed by atomic force microscopy (AFM). (**A**) Overview of adhesion forces between *S. mutans* UA159– and *S. sanguinis* SK 36–functionalized probes and collagen substrates at 0- and 5-s contact times. Values are presented as median, interquartile range, and 95% CI. (**B**) Histograms for 5-s contact time adhesion forces between streptococcal-functionalized probes and collagen substrates. Insets illustrate 2 representative retraction curves per condition, in which individual unbinding events can be observed. $n = 250$ force-distance curves per contact time across 3 independent gels per group. ****$P < 0.0001$. Kruskal-Wallis test. MGO, methylglyoxal; PBS, phosphate-buffered saline.

data suggest that glycation-induced crosslinking increases the mechanical stiffness of individual collagen fibrils. This is biologically relevant, as crosslinks act as merging blocks between collagen molecules; therefore, an increase in the number of crosslinks within the collagen leads to higher elastic modulus values within the matrix (Reddy 2004), which in human tissues has been associated with aging, diabetes, and other collagen genetic diseases (Snedeker and Gautieri 2014).

Streptococcal Nanoadhesion to Collagen Surfaces Is Modulated by Glycation

In recent years, nanotechnological approaches such as AFM have allowed researchers to study the topography and mechanical properties of biological samples at nanoscale resolution (Dufrêne et al. 2017). AFM has also been shown to be a suitable technique to explore the adhesion of bacteria onto surfaces (Alsteens et al. 2013), which is the critical initial step in the process of biofilm formation (Hojo et al. 2009). Thus, the real-time attachment of single *S. mutans* UA159 and *S. sanguinis* SK 36 cells to control and collagen surfaces was explored with AFM (Fig. 3). Low loading forces of 200 pN were employed to minimize the compression of bacteria onto collagen and reflect the true biological interaction between planktonic cells and surfaces. For *S. mutans* UA159 and *S. sanguinis* SK 36, increasing the contact time from 0 to 5 s resulted in increased adhesion forces, which suggests time-dependent bond maturation between bacteria and collagen fibrils. Furthermore, single unbinding events indicative of single adhesin-surface detachment could be observed at both contact times, suggesting an interaction between streptococcal collagen adhesins (Ajdic et al. 2002; Xu et al. 2007) and collagen surfaces (observed as "sawtooth" patterns in Fig. 3B, insets; Aguayo et al. 2016). In recent work, Wang et al. (2019) explored the adhesion of *S. mutans* to several hard substratum surfaces using a similar AFM approach, employing loading forces of 5 nN. We found reduced adhesion forces between streptococci and collagen as compared with those reported by

Wang et al., which could be a result of the reduced loading forces (200 pN) and the softer and fibrillar nature of collagen scaffolds as compared with hard substrates.

The studied bacterial strains differed in their adhesion behavior to collagen substrates. *S. mutans* UA159 significantly increased its attachment forces to glucose- and MGO-modified collagen surfaces as compared with the control. Furthermore, adhesion to MGO had a bimodal distribution, with a second peak around 0.5 nN. This effect could be explained by the changes in the topography of MGO-treated collagen that increase surface contact between the bacterium and substrate; however, as this effect was not observed for *S. sanguinis* SK 36, it remains possible that the increased glycation of collagen fibrils specifically promotes *S. mutans* UA159 adhesion onto the surface (e.g., via specific substrate-adhesin interactions). However, *S. sanguinis* SK 36 adhered more strongly to control collagen surfaces, whereas glucose and MGO modification significantly reduced cell surface attachment forces. This stronger adhesion of a *S. sanguinis* strain to collagen suggests that commensal initial colonizers may have an overall higher affinity to collagen at the nanoscale level as compared with other oral streptococcal species such as *S. mutans* UA159. Similar results were observed in the literature, as *S. sanguinis* was found to attach stronger to dental implant surfaces as compared with *Staphylococcus aureus*, an important pathogen in implant-related disease (Aguayo et al. 2015, 2016). Overall, it appears that type I collagen glycation favors the adhesion of *S. mutans* UA159 onto collagen fibrils and reduces adhesion forces between *S. sanguinis* SK 36 and the collagen matrix at the nanoscale level. These new findings could be especially interesting for the balance between these species on dentin surfaces and subsequent biofilm dysbiosis in the context of age-related collagen changes (Pitts et al. 2017).

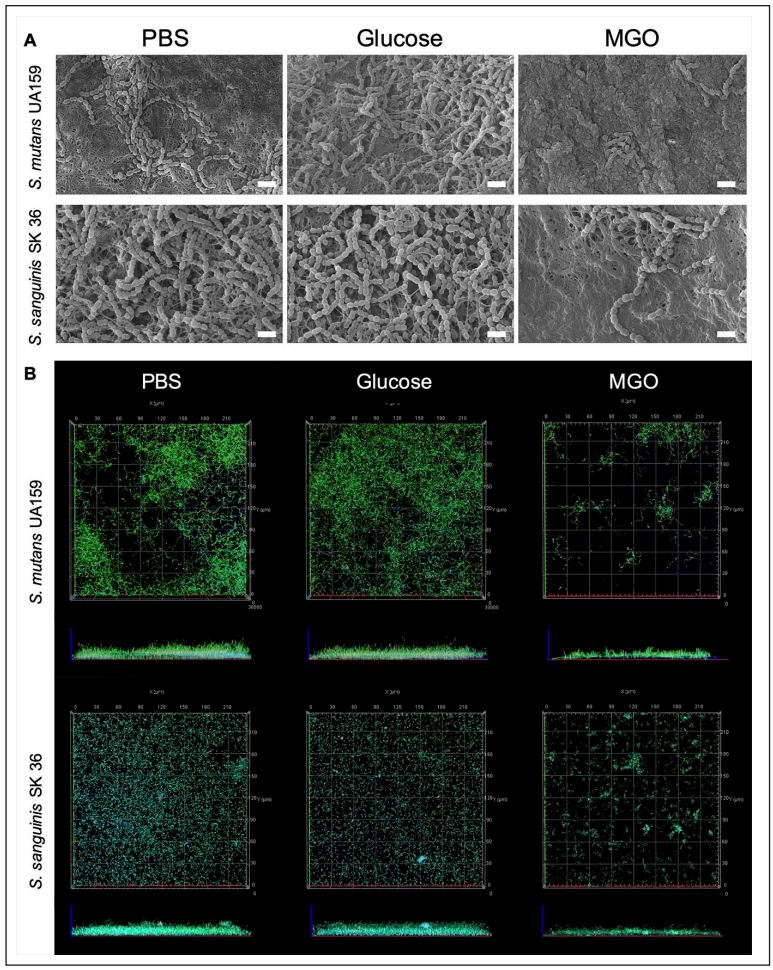

Figure 4. Streptococcal biofilm formation on collagen substrates is influenced by collagen crosslinking. (**A**) Scanning electron microscopy images of *Streptococcus mutans* UA159 and *Streptococcus sanguinis* SK 36 24-h biofilms on the surface of control, glucose-, and MGO-treated collagen substrates (scale bar = 2 µm). (**B**) Top (250 × 250–µm scans) and lateral (z = 30 µm) confocal laser scanning microscopy 3-dimensional reconstructions of 24-h streptococcal biofilms bound to collagen surfaces. Green, SYTO9; blue, Cascade Blue Dextran; red, propidium iodide. MGO, methylglyoxal; PBS, phosphate-buffered saline.

Effect of Crosslinking on Early Biofilm Formation and EPS Production

Imaging of biofilms revealed an intimate interaction between the bacteria and collagen fibrils, some of which penetrated into the collagen gel subsurface (Fig. 4A). Furthermore, confocal laser scanning microscopy imaging showed increased *S. mutans* UA159 biofilm formation on glucose-crosslinked surfaces, while MGO crosslinking reduced biofilm formation for both studied strains (Fig. 4B). Crystal violet assays showed that glucose-induced crosslinking increased biofilm formation in *S. mutans* UA159 by about 20%, while no significant change was seen for *S. sanguinis* SK 36 (Fig. 5A). These data are consistent with AFM results showing an increase in the adhesion forces between *S. mutans* UA159 and glucose-modified collagen. However, for both strains, the MGO-modified surface displayed notable reductions (~50%) in biofilm formation, which could be explained by the reduced surface roughness of the MGO-modified collagen (Appendix Fig. 1) and which would likely diminish retention of biofilms on the collagen substrate.

To explore the potential modulation of collagen changes on biofilm EPS production, IEPS and SEPS were extracted and quantified from 24-h biofilms (Fig. 5B). Overall, both strains produced higher levels of SEPS as compared with IEPS. For *S. mutans*, there was a significant increase in SEPS content in glucose-treated collagen as compared with control collagen gels ($P < 0.05$), which could explain the increase in biofilm biomass previously observed. Confocal laser scanning microscopy EPS quantification of fluorescent-labeled dextran demonstrated that streptococci attached to MGO-treated surfaces exhibit reduced EPS production (Fig. 5C).

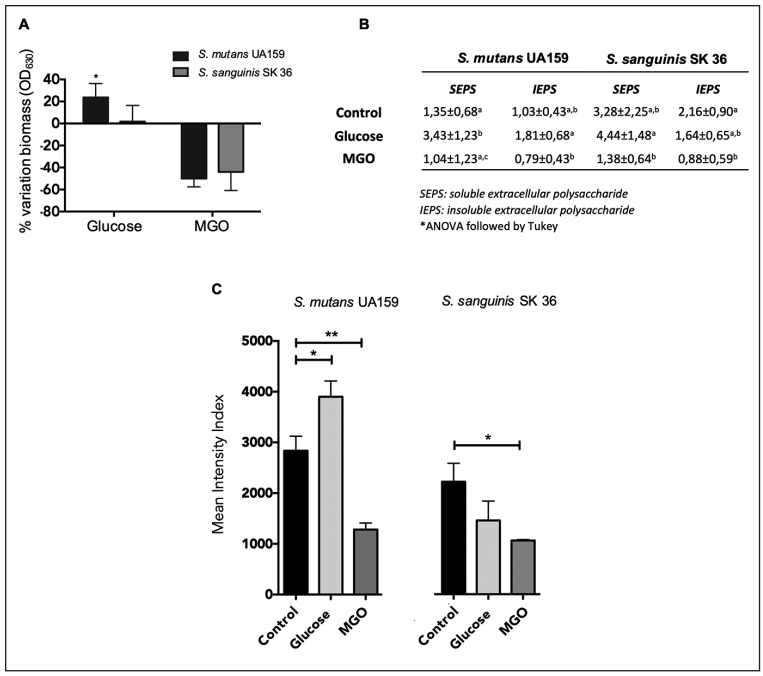

Figure 5. EPS secretion by 24-h biofilms adhered to control, glucose-, or MGO-treated surfaces. (**A**) Percentage variation of biomass as compared with collagen controls, determined by crystal violet staining. $n = 3$. Three technical replicates per group. $^{*}P < 0.05$. Analysis of variance. (**B**) Soluble and insoluble EPS quantification on control and crosslinked collagen surfaces. Values are presented mean ± SD. $n = 5$. Three technical replicates per group per independent *n*. (**C**) Mean intensity index for EPS (Cascade Blue dextran) for *Streptococcus mutans* UA159 and *Streptococcus sanguinis* SK 36 bound to collagen surfaces, measured across the basal region of each biofilm. $n = 3$. $^{*}P < 0.05$. $^{**}P < 0.01$. Analysis of variance. EPS, extracellular polysaccharide substance; MGO, methylglyoxal.

Overall, it appears that mild glycation of collagen surfaces promotes initial adhesion, biofilm formation, and IEPS production by *S. mutans* UA159, with no such effect observed for *S. sanguinis* SK 36. This suggests that glucose-induced crosslinking of collagen surfaces may be an important factor in promoting *S. mutans* over nonacidogenic streptococci such as *S. sanguinis*, which has been proposed as an important component in the progression of dental caries (Guo et al. 2019), and further work should explore how collagen glycation affects the *S.mutans/S. sanguinis* ratios within the biofilm. Also, nanoadhesion data revealed a reduction in the initial interaction between *S. sanguinis* SK 36 and glycated surfaces, which could promote this unbalance. This observation has potential biological repercussions, as dentinal collagen glycation may play an important role in the pathogenesis of dental caries observed in older people and patients with diabetes.

However, MGO-mediated glycation generated a quick and robust incorporation of crosslinks into the collagen matrix that altered the topography and mechanical properties of collagen fibrils and reduced biofilm formation for both streptococcal strains. Thus, it is believed that MGO treatment does not fully represent the gradual physiologic process of collagen crosslinking; however, it could be used as a simplified in vitro model for chemical crosslinking. Some studies have described that inducing dentin crosslinking with chemical agents such as proanthocyanidin and riboflavin improved acid resistance and collagen stability, thus concluding that chemical crosslinking can increase resistance to dental caries (Walter et al. 2008; Uemura et al. 2019). Our current work suggests that the chemical crosslinking of collagen is also able to reduce streptococcal biofilm formation and may therefore increase the resistance of chemically crosslinked dentin to dental caries. Future work should focus on the use of mutant strains deficient on specific collagen-binding receptors or purified collagen-binding proteins to elucidate the molecular mechanisms behind streptococcal adhesion to collagen surfaces.

Conclusion

An in vitro collagen glycation and crosslinking model has effectively been characterized and optimized to explore the early adhesion and biofilm formation of *S. mutans* UA159 and *S. sanguinis* SK 36. Glucose and MGO induced micro- and nanoscale morphologic and mechanical changes in collagen fibrils, increasing the elastic modulus. Overall, glucose-derived AGEs specifically promoted the initial adhesion, biofilm formation, and IEPS production of *S. mutans* UA159, while MGO treatment reduced biofilm formation on surfaces. Changes in the adhesion behavior and biofilm formation of oral streptococci as a function of collagen glycation may help explain the increased dysbiosis seen in older people and patients with diabetes. Furthermore, understanding the influence of collagen crosslinking on the balance between acidogenic and nonacidogenic streptococci may aid in developing novel preventive and therapeutic treatment against dental caries in these patients.

Author Contributions

C.M.A.P. Schuh, contributed to design, data acquisition, and interpretation, drafted and critically reviewed the manuscript; B. Benso, contributed to data acquisition and interpretation, critically reviewed the manuscript; P.A. Naulin, contributed to design and data acquisition, critically reviewed the manuscript; N.P. Barrera, L. Bozec, contributed to design and data interpretation, critically reviewed the manuscript; S. Aguayo, contributed to conception, design, data acquisition, and interpretation, drafted and critically reviewed the manuscript. All authors gave final approval and agree to be accountable for all aspects of the work.

Acknowledgments

The authors thank the Pharmacology and Toxicology Laboratory, School of Dentistry, UNICAMP (Brazil), for kindly providing the bacterial strains used in this study; Dr. Patricio Smith for providing some of the reagents for collagen glycation; and Rocío Orellana for her technical assistance during collagen gel SEM

processing. This work was funded by a FONDECYT Iniciación grant (11180101). The authors declare no potential conflicts of interest with respect to the authorship and/or publication of this article.

ORCID iDs

C.M.A.P. Schuh https://orcid.org/0000-0001-9475-4513
B. Benso https://orcid.org/0000-0002-4425-5174
S. Aguayo https://orcid.org/0000-0003-0900-1993

References

Aguayo S, Donos N, Spratt D, Bozec L. 2015. Nanoadhesion of *Staphylococcus aureus* onto titanium implant surfaces. J Dent Res. 94(8):1078–1084.
Aguayo S, Donos N, Spratt D, Bozec L. 2016. Probing the nanoadhesion of *Streptococcus sanguinis* to titanium implant surfaces by atomic force microscopy. Int J Nanomedicine. 11:1443–1450.
Ajdic D, McShan WM, McLaughlin RE, Savic G, Chang J, Carson MB, Primeaux C, Tian R, Kenton S, Jia H, et al. 2002. Genome sequence of *Streptococcus mutans* UA159, a cariogenic dental pathogen. Proc Natl Acad Sci U S A. 99(22):14434–14439.
Akhshabi S, Biazar E, Singh V, Keshel SH, Geetha N. 2018. The effect of the carbodiimide cross-linker on the structural and biocompatibility properties of collagen–chondroitin sulfate electrospun mat. Int J Nanomedicine. 13:4405–4416.
Alsteens D, Beaussart A, El-Kirat-Chatel S, Sullan RMA, Dufrêne YF. 2013. Atomic force microscopy: a new look at pathogens. PLoS Pathog. 9(9):e1003516.
Avilés-Reyes A, Miller JH, Lemos JA, Abranches J. 2017. Collagen-binding proteins of *Streptococcus mutans* and related streptococci. Mol Oral Microbiol. 32(2):89–106.
Chong SAC, Lee W, Arora PD, Laschinger C, Young EWK, Simmons CA, Manolson M, Sodek J, McCulloch CA. 2007. Methylglyoxal inhibits the binding step of collagen phagocytosis. J Biol Chem. 282(11):8510–8520.
Clinical and Laboratory Standards Institute. 2014. Performance Standards for Antimicrobial Susceptibility Testing; Twenty-Fourth Informational Supplement. CLSI.
Collier TA, Nash A, Birch HL, de Leeuw NH. 2016. Intra-molecular lysine-arginine derived advanced glycation end-product cross-linking in type I collagen: a molecular dynamics simulation study. Biophys Chem. 218:42–46.
Donlan RM. 2002. Biofilms: microbial life on surfaces. Emerg Infect Dis. 8(9):881–890.
DuBois M, Gilles KA, Hamilton JK, Rebers PA, Smith F. 1956. Colorimetric method for determination of sugars and related substances. Anal Chem. 28(3):350–356.
Dufrêne YF, Ando T, Garcia R, Alsteens D, Martinez-Martin D, Engel A, Gerber C, Müller DJ. 2017. Imaging modes of atomic force microscopy for application in molecular and cell biology. Nat Nanotechnol. 12(4):295–307.
Flemming H-C, Wingender J. 2010. The biofilm matrix. Nat Rev Microbiol. 8(9):623–633.
Francis-Sedlak ME, Uriel S, Larson JC, Greisler HP, Venerus DC, Brey EM. 2009. Characterization of type I collagen gels modified by glycation. Biomaterials. 30(9):1851–1856.
Gelse K, Pöschl E, Aigner T. 2003. Collagens—structure, function, and biosynthesis. Adv Drug Deliv Rev. 55(12):1531–1546.
Greis F, Reckert A, Fischer K, Ritz-Timme S. 2018. Analysis of advanced glycation end products (AGEs) in dentine: useful for age estimation? Int J Legal Med. 132(3):799–805.
Guo X, Liu S, Zhou X, Hu H, Zhang K, Du X, Peng X, Ren B, Cheng L, Li M. 2019. Effect of D-cysteine on dual-species biofilms of *Streptococcus mutans* and *Streptococcus sanguinis*. Sci Rep. 9(1):6689.
Hojo K, Nagaoka S, Ohshima T, Maeda N. 2009. Bacterial interactions in dental biofilm development. J Dent Res. 88(11):982–990.
Kassebaum NJ, Bernabé E, Dahiya M, Bhandari B, Murray CJL, Marcenes W. 2014. Global burden of severe tooth loss. J Dent Res. 93(7):20S–28S.
Kreth J, Merritt J, Qi F. 2009. Bacterial and host interactions of oral streptococci. DNA Cell Biol. 28(8):397–403.
Loesche WJ. 1986. Role of *Streptococcus mutans* in human dental decay. Microbiol Rev. 50(4):353–380.
Marsh PD. 1994. Microbial ecology of dental plaque and its significance in health and disease. Adv Dent Res. 8(2):263–271.
Nass N, Bartling B, Santos AN, Scheubel RJ, Börgermann J, Silber RE, Simm A. 2007. Advanced glycation end products, diabetes and ageing. Z Gerontol Geriatr. 40(5):349–356.
Nevin C, McNeil L, Ahmed N, Murgatroyd C, Brison D, Carroll M. 2018. Investigating the glycating effects of glucose, glyoxal and methylglyoxal on human sperm. Sci Rep. 8(1):9002.
Oliveira BEC, Cury JA, Filho APR. 2017. Biofilm extracellular polysaccharides degradation during starvation and enamel demineralization. PLoS One. 12(7):e0181168.
Pitts NB, Zero DT, Marsh PD, Ekstrand K, Weintraub JA, Ramos-Gomez F, Tagami J, Twetman S, Tsakos G, Ismail A. 2017. Dental caries. Nat Rev Dis Prim. 3:17030.
Reddy GK. 2004. Cross-linking in collagen by nonenzymatic glycation increases the matrix stiffness in rabbit Achilles tendon. Exp Diabetes Res. 5(2):143–153.
Sato Y, Okamoto K, Kagami A, Yamamoto Y, Igarashi T, Kizaki H. 2004. *Streptococcus mutans* strains harboring collagen-binding adhesin. J Dent Res. 83(7):534–539.
Schuh CMAP, Aguayo S, Zavala G, Khoury M. 2019. Exosome-like vesicles in *Apis mellifera* bee pollen, honey and royal jelly contribute to their antibacterial and pro-regenerative activity. J Exp Biol. 222:jeb208702.
Shinno Y, Ishimoto T, Saito M, Uemura R, Arino M, Marumo K, Nakano T, Hayashi M. 2016. Comprehensive analyses of how tubule occlusion and advanced glycation end-products diminish strength of aged dentin. Sci Rep. 6:19849.
Snedeker JG, Gautieri A. 2014. The role of collagen crosslinks in ageing and diabetes—the good, the bad, and the ugly. Muscles Ligaments Tendons J. 4(3):303–308.
Switalski LM, Butcher WG, Caufield PC, Lantz MS. 1993. Collagen mediates adhesion of *Streptococcus mutans* to human dentin. Infect Immun. 61(10):4119–4125.
Takahashi N, Nyvad B. 2008. Caries ecology revisited: microbial dynamics and the caries process. Caries Res. 42(6):409–418.
Takahashi N, Nyvad B. 2016. Ecological hypothesis of dentin and root caries. Caries Res. 50(4):422–431.
Uemura R, Miura J, Ishimoto T, Yagi K, Matsuda Y, Shimizu M, Nakano T, Hayashi M. 2019. UVA-activated riboflavin promotes collagen crosslinking to prevent root caries. Sci Rep. 9(1):1252.
Vos T, Abajobir AA, Abbafati C, Abbas KM, Abate KH, Abd-Allah F, Abdulle AM, Abebo TA, Abera SF, Aboyans V, et al; GBD 2016 Disease and Injury Incidence and Prevalence Collaborators. 2017. Global, regional, and national incidence, prevalence, and years lived with disability for 328 diseases and injuries for 195 countries, 1990–2016: a systematic analysis for the Global Burden of Disease Study 2016. Lancet. 390(10100):1211–1259. Erratum in: Lancet. 2017;390(10106):e38.
Walter R, Miguez PA, Arnold RR, Pereira PNR, Duarte WR, Yamauchi M. 2008. Effects of natural cross-linkers on the stability of dentin collagen and the inhibition of root caries in vitro. Caries Res. 42(4):263–268.
Wang C, Hou J, van der Mei HC, Busscher HJ, Ren Y. 2019. Emergent properties in *Streptococcus mutans* biofilms are controlled through adhesion force sensing by initial colonizers. Brennan RG, editor. mBio. 10(5):e01908-19.
Xu P, Alves JM, Kitten T, Brown A, Chen Z, Ozaki LS, Manque P, Ge X, Serrano MG, Puiu D, et al. 2007. Genome of the opportunistic pathogen *Streptococcus sanguinis*. J Bacteriol. 189(8):3166–3175.
Zheng L, Itzek A, Chen Z, Kreth J. 2011. Oxygen dependent pyruvate oxidase expression and production in *Streptococcus sanguinis*. Int J Oral Sci. 3(2):82–89.
Zhu B, Macleod LC, Kitten T, Xu P. 2018. *Streptococcus sanguinis* biofilm formation and interaction with oral pathogens. Future Microbiol. 13(8):915–932.